Short Communication

Effect of partial substitution of La with Ce, Pr and Nd on the properties of LaNi$_5$-based alloy electrodes

J. Chen, S.X. Dou, H.K. Liu

Institute for Materials Technology and Manufacturing, University of Wollongong, Northfields Avenue, Wollongong, NSW 2522, Australia

Abstract

A comparison is made of the properties of LaB$_5$ (B = Ni$_{3.55}$Co$_{0.75}$Mn$_{0.4}$Al$_{0.3}$), La$_{0.7}$R$_{0.3}$B$_5$ (R = Ce, Pr, Nd) and MmB$_5$ (Mm is mischmetal in an atomic ratio of La:Ce:Pr:Nd = 0.7:0.2:0.05:0.05) alloy electrodes. X-ray diffraction results reveal that Ce, Pr, Nd substitute for La and decrease the unit cell volume. Pressure–composition isotherms of the electrode alloys are determined by an electrochemical method. The characteristics of the alloy electrodes, including initial activation, high-rate discharge, cycle life and self-discharge, are examined. It is found that partial replacement of La with Ce, Pr, Nd in the LaNi$_5$-based alloy improves greatly the activation, high-rate discharge and cycle life of the electrode, but increases the self-discharge due to a higher dissociation pressure of the metal hydride.

Keywords: Lanthanum–nickel-based alloy; Substitution; Hydride electrodes

1. Introduction

Since the early 1990s, hydrogen-storage alloys have attracted attention as electrode materials for reversible hydrogen storage in nickel/metal-hydride (Ni/MH) batteries. These alloys possess both environmental and technical advantages over the cadmium electrode [1–4]. To develop a useful metal hydride electrode, however, the capacity loss of the electrode at high-rate charge/discharge cycling must be overcome [5,6].

The main causes for the capacity loss of metal-hydride electrodes are: (i) oxidation of the alloy by oxygen that is evolved on the nickel electrode either at high-rate charge or at the end of the charge; (ii) oxidation of the new alloy surface that is produced by the disintegration of the alloy caused by hydrogen absorption/desorption in the electrolytic solution; (iii) adverse effects of the outside oxidized layer in both losing hydrogen-storage capacity and hindering the diffusion of hydrogen when the electrode is charged or discharged.

In order to solve these problems, work has been directed towards finding improved hydride materials such as LaNi$_5$-based and MmNi$_5$ (Mm is mischmetal) multicomponent alloys [7,8]. Mischmetal is widely adopted because of its low cost [9,10]. While the effects of Ni substitution have been studied in detail, little attention has been focused on the influence of La partial replacement on electrode performance.

In this study, an LaNi$_5$-based alloy has been modified by partial substitution of La with Ce, Pr and Nd in order to investigate the effect on the unit cell volume, the de-hydriding plateau pressure, and the charge/discharge characteristics.

2. Experimental

2.1. Alloy preparation

The alloys of LaB$_5$, La$_{0.7}$R$_{0.3}$B$_5$ and MmB$_5$ were prepared from pure components by arc melting under a purified argon atmosphere. All the metal materials (purity $\geq$ 99.9%) were provided by the Aldrich Chemical Company. After the first melt, the ingot was melted a further three times in order to achieve complete homogeneity. The ingots were annealed at 950 °C for 24 h under a pressure of 10^{-2} torr. After cooling to room temperature, the ingots were pulverized by ball milling under an argon atmosphere. X-ray diffraction (XRD) was used to examine the phase structure and lattice parameters.

2.2. Electrode preparation

A 0.5 g sample of alloy powder (about 40 μm) and 0.5 g of nickel powder (3 μm) were mixed thoroughly and then pressed mechanically into a pellet (diameter: 1.0 cm) under

a pressure of 3×10^6 Pa. The pellet was then sandwiched in a nickel foam that was attached to a nickel wire for electrical connection.

2.3. Electrochemical measurements

The electrode properties were evaluated at a controlled temperature by using a divided electrochemical cell. A Hg/HgO reference electrode and an Ni(OH)$_2$ positive electrode were employed. The electrolyte was 5 M KOH. The performance of each electrode was examined by an automative galvanostatic charge/discharge unit (DEC-1). When discharged, a maximum potential of -740 mV versus Hg/HgO was adopted. Hydrogen pressure–composition isotherms (P–C–T curves) were measured by an electrochemical method.

3. Results and discussion

3.1. Phase structure

The LaB$_5$, La$_{0.7}$R$_{0.3}$B$_5$ and MmB$_5$ alloys were analysed by XRD, all the samples have the same hexagonal CaCu$_5$ structure. The unit cell volumes of the alloys are presented in Table 1. It can be seen that LaB$_5$ alloy has the largest unit cell volume (i.e. the largest a but the smallest c), the La$_{0.7}$Nd$_{0.3}$B$_5$ alloy has the smallest unit cell volume (i.e. the smallest a but the largest c). Thus, partial substitution of La with Ce, Pr and Nd results in a decrease in the unit cell volume of the alloy. This contraction implies a smaller interstitial volume and hence, a larger distortion when hydrogen occupies an interstitial site [11]. The hydriding/de-hydriding pressure will also be higher for the system with a smaller unit cell volume. This is confirmed in the study reported here.

3.2. Activation of the electrode

The LaB$_5$, La$_{0.7}$R$_{0.3}$B$_5$ and MmB$_5$ alloy electrodes are activated as follows: charged at 30 mA (0.2C rate) for 7 h and discharged at 30 mA to -740 mV versus Hg/HgO. The capacity versus cycle number performances are shown in Fig. 1. The La$_{0.7}$Ce$_{0.3}$B$_5$ electrode exhibits the fastest activation (after 5 cycles, the capacity is 315 mAh g^{-1}), while the LaB$_5$ electrode has the slowest activation (after 5 cycles,
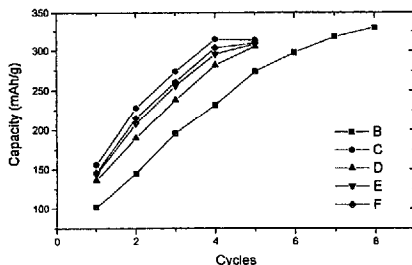
Table 1
Unit-cell volume of alloys

Alloy	a (Å)	c (Å)	c/a	Volume (Å^3)
LaB$_5$	5.063	4.031	0.7962	89.48
La$_{0.7}$Ce$_{0.3}$B$_5$	5.032	4.046	0.8040	88.72
La$_{0.7}$Pr$_{0.3}$B$_5$	5.016	4.052	0.8078	88.29
La$_{0.7}$Nd$_{0.3}$B$_5$	5.002	4.056	0.8108	87.88
MmB$_5$	5.018	4.050	0.8071	88.31

Fig. 1. Initial activation of the alloy electrodes: (B) LaB$_5$; (C) La$_{0.7}$Ce$_{0.3}$B$_5$; (D) La$_{0.7}$Pr$_{0.3}$B$_5$; (E) La$_{0.7}$Nd$_{0.3}$B$_5$, and (F) MmB$_5$.

the capacity is 262 mAh g^{-1}). Thus, substitution of La by Ce, Pr and Nd greatly improves the hydrogen absorption/desorption (charge/discharge) kinetics of the alloys. This may be due to an increase in the c dimension of the unit cell, which possibly increases the rate of diffusion of hydrogen through the hydride.

3.3. Electrochemical P–C–T curves

According to Ref. [12], when the electrolyte is 5 M KOH, the potential of the metal hydride electrode versus Hg/HgO can be calculated via the following equations:

$$0°\,C:\ E(V) = -0.9364 - 0.0271 \log p(H_2) \quad (1)$$

$$25°\,C:\ E(V) = -0.9293 - 0.0296 \log p(H_2) \quad (2)$$

$$40°\,C:\ E(V) = -0.9248 - 0.0310 \log p(H_2) \quad (3)$$

The pressure–composition desorption (discharging) isotherms for the activated LaB$_5$, La$_{0.7}$R$_{0.3}$B$_5$ and MmB$_5$ alloys are shown in Fig. 2. Partial substitution of La by Ce, Pr and Nd increases the plateau pressure (hydride desorption) of the alloy. It should also be noted that there is a decrease in hydrogen-storage capacity (i.e. the maximum discharge capacity, mAh g^{-1}) with Ce, Pr, Nd substitution. For example, Fig. 2(b) indicates that the LaB$_5$ alloy has the maximum discharge capacity (330 mAh g^{-1} at 25 °C); the others are about 310 mAh g^{-1}.

The thermodynamics of the alloy-hydrogen reaction can be conveniently represented by the van 't Hoff equation, which is a plot of the dissociation pressures versus the reciprocal of the absolute temperature [13]. The calculated enthalpy for the formation of the metal hydride are listed in Table 2. The stability of these hydrides is in the order:

LaB$_5$ > La$_{0.7}$Pr$_{0.3}$B$_5$ > La$_{0.7}$Nd$_{0.3}$B$_5$ > MmB$_5$ > La$_{0.7}$Ce$_{0.3}$B$_5$

This finding agrees with the previously reported results of Clay et al. [14].

3.4. High-rate discharge

After activation, the LaB$_5$, La$_{0.7}$R$_{0.3}$B$_5$ and MmB$_5$ electrodes were charged at 30 mA for 7 h and discharged in the
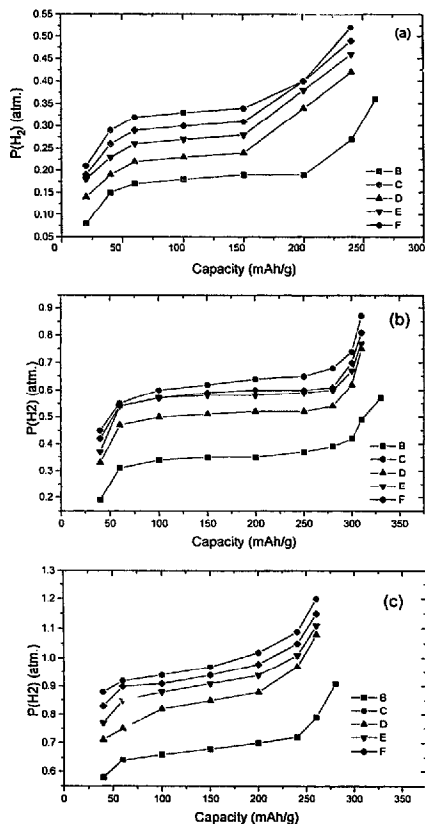
Fig. 2. Electrochemical P–C–T curves for the electrode alloys at temperature of: (a) 0 °C; (b) 25 °C, and (c) 40 °C. (B) LaB₅; (C) La₀.₇Ce₀.₃B₅; (D) La₀.₇Pr₀.₃B₅; (E) La₀.₇Nd₀.₃B₅, and (F) MmB₅.

30–150 mA current range (0.2–1C rate). The discharge capacities of the electrode alloys are listed in Table 3. The result shows that the La₀.₇Ce₀.₃B₅ alloy has the best high-rate discharge and the LaB₅ alloy the lowest.

3.5. Cycle life

The cycle life of the LaB₅, La₀.₇R₀.₃B₅ and MmB₅ electrodes was evaluated under the following conditions: (i) charge: 150 mA for 1.2 h; (ii) discharge: 150 mA for 1 h, and (iii) temperature: 20–25 °C. The results reveal (Fig. 3) that there is a rapid increase in capacity during the first few cycles, this is due to an activation process. After activation, a maximum discharge capacity is reached and then the capac-

Table 2
Plateau pressure (p_{eq} at 25 °C), enthalpy ($-\Delta H$) and entropy ($-\Delta S$) for alloys

Alloy	p_{eq}	$-\Delta H$	$-\Delta S$
	(atm)	(kJ/mol H₂)	(J/(mol H₂ K))
LaB₅	0.35	39.7	128
La₀.₇Ce₀.₃B₅	0.64	36.8	106
La₀.₇Pr₀.₃B₅	0.52	38.9	121
La₀.₇Nd₀.₃B₅	0.58	38.0	123
MmB₅	0.60	37.2	110

Table 3
High-rate discharge capacity of alloy electrodes

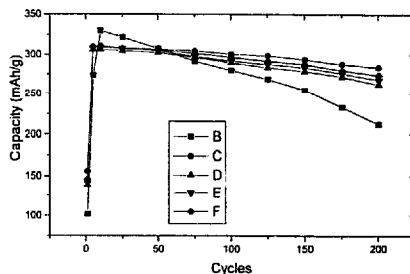| Discharge current	Capacity (mAh g⁻¹)				
	1	2	3	4	5
30 mA (0.2C)	330	315	306	310	308
60 mA (0.4C)	294	301	278	282	279
150 mA (1C)	247	276	248	260	258
C_{150}/C_{30}	74.8	87.9	81.0	83.9	83.8

Fig. 3. Cycle life of alloy electrodes; (B) LaB₅; (C) La₀.₇Ce₀.₃B₅; (D) La₀.₇Pr₀.₃B₅; (E) La₀.₇Nd₀.₃B₅, and (F) MmB₅.

ity decreases. The LaB₅ alloy displays the fastest decline in capacity, the La₀.₇Ce₀.₃B₅ alloy the slowest. The capacity decay can be explained by corrosion of the electrodes [15]. The latter is determined not only by the change in unit cell volume, but also by the rare-earth composition. The presence of a small amount of Ce has been shown to retard corrosion, possibly because Ce can form a protective oxide film (CeO₂) on the alloy surface.

3.6. Self-discharge

The charge retention of the electrodes was examined at 20 °C (charge: 30 mA for 7 h; rest for 2 days; discharge: 30 mA to −740 mV versus Hg/HgO). The results are presented in Table 4. It can be concluded that the higher is the dissociation pressure, the higher is the self-discharge of the alloy electrode. There are two kinds of self-discharge, namely, reversible and irreversible. The former is caused by the high

Table 4
Self-discharge of electrodes after 2 days of storage

Electrode	C_{max} [a] $(mAh\,g^{-1})$	C_{ret} [b] $(mAh\,g^{-1})$	$C_{max}-C_{ret}$	Self-discharge [c] (%)
LaB$_5$	330	288	42	12.7
La$_{0.7}$Ce$_{0.3}$B$_5$	315	251	64	20.3
La$_{0.7}$Pr$_{0.3}$B$_5$	306	253	53	17.3
La$_{0.7}$Nd$_{0.3}$B$_5$	310	260	50	16.1
MmB$_5$	308	250	58	18.8

[a] C_{max}: maximum capacity.

[b] C_{ret}: capacity retained after 2 days of storage.

[c] Self-discharge (%) $\approx [(C_{max}-C_{ret})\div C_{max}] \times 100\%$.

dissociation pressure of the metal hydride, the latter by the oxidation of the alloy [16]. Although the La$_{0.7}$Co$_{0.3}$B$_5$ alloy electrode has the highest self-discharge, the main cause is the reversible process. For the LaB$_5$ electrode, however, self-discharge is mainly produced by the irreversible process.

4. Conclusions

From the above results, it can be summarized that partial substitution of La by Ce, Pr and Nd in the LaNi$_5$-based hydrogen-storage alloy: (i) has no effect on the hexagonal CaCu$_5$ structure, but changes the lattice parameters; (ii) improves the electrode's activation, high-rate discharge and cycle life, but decreases the discharge capacity by about 20 mAh g^{-1}, and (iii) increases the self-discharge of the electrode due to the higher dissociation pressure of the metal hydride.

It also can be concluded that La$_{0.7}$Ce$_{0.3}$B$_5$ has the best overall performance. Therefore, in the manufacturing process of this metal hydride electrode, the content of each rare-earth in the mischmetal should be controlled accurately.

References

[1] T. Sakai, A. Yuasa, H. Ishikawa, H. Miyamura and N. Kuriyama, *J. Less-Common Met.*, *172–174* (1991) 1194.

[2] A. Anani, A. Visintin, K. Petrov and S. Srinivasan, *J. Power Sources*, *47* (1994) 261.

[3] J. Chen and Y.S. Zhang, *Int. J. Hydrogen Energy*, *20* (1995) 235.

[4] B. Friedrich, *J. Mater. Eng. Performance*, *3* (1994) 37.

[5] J. Chen and Y.S. Zhang, *J. Mater. Res.*, *9* (1994) 1802.

[6] B. Luan, N. Cui, H. Zhao, H.K. Liu and S.X. Dou, *J. Power Sources*, *55* (1995) 101.

[7] J.J.G. Willems and K.H. Buschow, *J. Less-Common Met.*, *129* (1987) 287.

[8] T. Sakai, T. Hazama, H. Miyamura, N. Kuriyama, A. Kato and H. Ishikawa, *J. Less-Common Met.*, *172–174* (1991) 1175.

[9] T. Sakai, H. Miyamura, N. Kuriyama, H. Ishikawa and I. Uehara, *J. Alloys Comp.*, *192* (1993) 155.

[10] G.D. Adzic, J.R. Johnson, J.J. Reilly, J. McBreen, S. Mukerjee, M.P. Sridhar Kumar, W. Zhang and S. Srinivasan, *J. Electrochem. Soc.*, *142* (1995) 3429.

[11] R. Balasubramaniam, M.N. Mungole and K.N. Rai, *J. Alloys Comp.*, *196* (1993) 63.

[12] J. Balej, *Int. J. Hydrogen Energy*, *10* (1985) 365.

[13] J.J. Reilly and R.H. Wiswall, *Inorg. Chem.*, *7* (1968) 2254.

[14] K.R. Clay, A.J. Goudy, R.G. Schweibanz and A. Zarynow, *J. Less-Common Met.*, *166* (1990) 153.

[15] A.J. Davenport, H.S. Isaas and M.W. Kendig, *Corros. Sci.*, *32* (1991) 653.

[16] C. Iwakura, Y. Kajiya, H. Yoneyama, T. Sakai, K. Oguro and H. Ishikawa, *J. Electrochem. Soc.*, *136* (1989) 1351.